

**TITLE: The Microtubule Network and Cell Death are Regulated by a miR-34a/Stathmin 1/ $\beta$ III-tubulin Axis**

**AUTHORS:** Nancy S. Vetter<sup>1</sup>, E. A. Kolb<sup>1</sup>, Christopher Mills<sup>2</sup>, Valerie B. Sampson<sup>1</sup>

**AFFILIATION:** <sup>1</sup>Nemours Center for Cancer and Blood Disorders, Nemours/Alfred I. duPont Hospital for Children, Wilmington, DE. <sup>2</sup>Department of Biological Sciences, University of Delaware, Newark, DE.

**CORRESPONDING AUTHOR:**

Valerie B. Sampson, PhD.

Nemours Center for Cancer and Blood Disorders,

A.I. duPont Hospital for Children,

1701 Rockland Road, Wilmington, DE. 19803

Email: vsampson@nemours.org

Phone: 302-651-4832

Fax: 301-651-4827

**RUNNING TITLE:** miR-34a targets *STMN1* mRNA in Osteosarcoma

**KEYWORDS:** miR-34a, stathmin1,  $\beta$ III-tubulin, microtubule destabilization, apoptosis, autophagy

**FINANCIAL SUPPORT:** This work is supported by the Clinical and Translational Research (CTR) Pilot Award to VS under grant number NIH U54-GM104941, the Cell Science Core of the Center for Pediatric Research which is supported by Institutional Development Awards (IDeA) under grant numbers P20GM103464 and P30GM114736 and the Biomolecular Core Lab which is supported by grants P20GM103464 (COBRE), P30GM114736 (COBRE) and P20GM103446 (INBRE).

**CONFLICT OF INTEREST:** The authors declare no potential conflicts of interest.

**WORD COUNT:** 5,082

**FIGURES (5) AND TABLES (2)**

## ABSTRACT

MicroRNA-34a (miR-34a) is a master regulator of signaling networks that maintain normal physiology and disease and is currently in development as a miRNA-based therapy for cancer. Prior studies have reported low miR-34a expression in osteosarcoma (OS); however, the molecular mechanisms underlying miR-34a activity in OS are not well defined. Therefore, this study evaluated the role of miR-34a in regulating signal transduction pathways that influence cell death in OS. Levels of miR-34a were attenuated in human OS cells and xenografts of the Pediatric Preclinical Testing Consortium (PPTC). Bioinformatics predictions identified stathmin 1 (STMN1) as a potential miR-34a target. Biotin pulldown assay and luciferase reporter analysis confirmed miR-34a target interactions within the STMN1 mRNA 3'UTR. Overexpression of miR-34a in OS cells suppressed STMN1 expression and reduced cell growth in vitro. Restoration of miR-34a led to microtubule destabilization and increased  $\beta$ III-tubulin expression, with corresponding G1/G2 phase cell cycle arrest and apoptosis. Knockdown of the Sp1 transcription factor, by siRNA silencing, also upregulated  $\beta$ III-tubulin expression in OS cells, suggesting miR-34a indirectly affects Sp1. Validating the coordinating role of miR-34a in microtubule destabilization, when miR-34a was combined with either microtubule inhibitors or chemotherapy, STMN1 phosphorylation was suppressed and there was greater cytotoxicity in OS cells. These results demonstrate that miR-34a directly represses STMN1 gene and protein expression and upregulates  $\beta$ III-tubulin, leading to disruption of the microtubule network and cell death.

Implications: The miR-34a/STMN1/ $\beta$ III-tubulin axis maintains the microtubule cytoskeleton in osteosarcoma, and combining miR-34a with microtubule inhibitors can be investigated as a novel therapeutic strategy.

## INTRODUCTION

Osteosarcoma (OS) is the most common bone tumor that occurs in children (1). About 70-75% of patients achieve a complete clinical response with multimodal therapy of standard chemotherapy and surgery. These treatments are ineffective for metastatic and relapsed disease. For patients with metastasis at diagnosis, the overall five-year survival rate is approximately 30% (2) and declines to 15% for those with recurrent OS (3). Rigorous preclinical studies are identifying novel agents and treatments that may lead to the development of new and effective therapies to improve survival outcomes for these patients. Understanding the molecular events that control disease progression and metastasis and how these affect drug response is essential for identifying agents that efficiently overcome mechanisms of drug resistance.

MicroRNAs (miRNAs) are a class of short, single-stranded, non-coding RNAs that are intricately involved in the post-transcriptional regulation of genes through messenger RNA (mRNA) silencing (4). These highly conserved RNAs contain 6–8 nucleotide seed sequences that bind mRNA 3' untranslated region (UTR) sequences. Full sequence complementarity of miRNA:mRNA binding is not required for miRNAs to function effectively (4), to promote transcript degradation and translational repression. A single miRNA can target and change the expression of many genes or many miRNAs can target a single gene. Several studies show that miRNAs have central roles in normal physiological processes as well as in pathological conditions, including cancer development and progression. Altered expression of specific miRNAs in cancer may predict prognosis and response to therapy (5). For example, high expression of the miR-200 family has been detected in ovarian cancer and is associated with early relapse and decreased overall survival (6). Expression signatures of local or systemically circulating miRNAs that are underexpressed (tumor suppressors) or highly expressed (oncogenes), can be developed as biomarkers for discriminating tumor origins, subtypes, and oncogenic mutations (7, 8). For miRNAs that function as tumor suppressors, miRNA mimics can be used to restore miRNA gene expression and inhibit target oncogenes.

MiR-34a is a master regulator of signaling networks that maintain normal physiology and disease and is in clinical development as a diagnostic, prognostic and therapeutic agent for several malignancies, including cancer. miR-34a belongs to an evolutionarily conserved miRNA family of genes which also contains miR-34b/c

and was first characterized as a cancer-related miRNA by Welch et al., in neuroblastoma (9). In their study (9), the encoding gene was mapped on chromosome 1p36.22. Gene deletions and rearrangements are frequently observed in the 1p36 region in a variety of human cancers including neuroblastoma, glioma, leukemia and breast cancer (10). In OS, 1p36 is a region of chromosomal gains with the amplified expression of several genes (11, 12). miR-34a was identified as an inhibitor of cancer cell growth in a wide range of solid and hematological malignancies (13, 14), including OS tumors (15, 16). Restoration of expression of miR-34a blocked cell migration, cell proliferation, and led to cell cycle arrest in G1 and G2 phase and apoptosis *in vitro* and *in vivo* in preclinical OS models (15, 17). Antitumor effects are mediated by repressing targets such as the transcription inducer of cell cycle progression E2F3 (E2F transcription factor 3), histone deacetylase sirtuin (SIRT1), cell cycle regulators, cyclin-dependent kinase 4/6 (CDK4, CDK6) and the anti-apoptotic protein B-cell lymphoma 2 (Bcl2) [reviewed in (13)]. Moreover, miR-34a is directly regulated by p53 transcriptional activation and epigenetic modulation, and inactivating mutations of p53 often correlate with the decrease in expression of miR-34a in tumors (18). The low frequency of minimal deletions for miR-34a in primary OS samples suggests that epigenetic alterations may play an important role in modulating the expression of miR-34a (15).

Stathmin 1 (STMN1), also known as oncoprotein 18 (Op18), is a microtubule-destabilizing protein that is ubiquitously expressed in vertebrates. The *STMN1* gene is located in the 1p36.11 chromosomal region and encodes a 19-kDa cytosolic phosphoprotein. STMN1 binds  $\beta$ -tubulin and regulates the dimerization and polymerization of tubulin (19). These are critical processes in the signaling cascade that controls the assembly and disintegration of the mitotic spindle during cell cycle progression, and cell movement. Dephosphorylation activates STMN1 for microtubule destabilization in interphase and cytokinesis, and phosphorylation deactivates STMN1 to allow microtubules to polymerize to form the mitotic spindle in prophase, and for cell movement (19, 20). Kumar et al. (21) identified STMN1 in bone cells and the protein was proposed to play a role in altering osteoblast growth and response to various hormonal stimuli. High STMN1 expression is frequently demonstrated in numerous types of cancer including acute leukemia, gastric and ovarian cancer (22-24) as well as OS (21, 25). Elevated STMN1 expression may represent one mechanism of resistance to the antitumor effects of microtubule inhibitors. STMN1 inhibition results in cell cycle arrest in the G2/M phase

and apoptosis, as well as the suppression of lung metastasis (25-27). Other studies show that resistance to docetaxel in gastric cancer is mediated via upregulation of STMN1 by FOXM1 transcription factor, and STMN1 knockdown inhibits *in vivo* tumor growth of gastric cancer cells (28). Overexpression of miR-31 in ovarian cancer restored sensitivity to chemotherapy by directly repressing STMN1 (29), and miR-101 also inhibited STMN1 and sensitized nasopharyngeal carcinoma cells to radiation (30).

The broad activity of miR-34a across several types of cancers suggests that miR-34a shares common molecular mechanisms of tumor suppression. Successful clinical application of this miRNA requires detailed knowledge of target gene regulation and a comprehensive understanding of the biological mechanism of action. In the current study, the mechanism of action of miR-34a in OS was investigated using a gain-of-function approach in p53-null and wild type-p53 human OS cell lines. We identified an association between miR-34a and STMN1 *in vitro* and evaluated the miR-34a signal transduction on STMN1 and pathways downstream involving the microtubule network. Our results highlight a novel regulatory pathway involving miR-34a, STMN1 and  $\beta$ III-tubulin that controls microtubule stability and dynamics, and mediates survival of OS cells.

## METHODS

**Cell culture:** Human OS cell lines SaOS (p53-null), 143B, HOS, U2OS (wild-type p53), MG-63 (mutant p53) and human osteoblasts (CRL-1132) were purchased from ATCC (Manassas, VA). SaOS and U2OS cells were cultured in McCoy's 5A medium, 143B, HOS and MG-63 cells in Modified Eagle's Medium (MEM) and osteoblasts in Ham's F12 Medium. Growth media were supplemented with 10% fetal bovine serum (FBS), 2 mM L-glutamine, 25 U/mL penicillin, and 25 µg/mL streptomycin. Cells were maintained at 37°C in humidified incubators, in an atmosphere of 5% CO<sub>2</sub>.

**OS xenograft tumors:** The OS1, OS2, OS9, OS17, OS31, OS33, OS46, OS51 and OS56 tumor lines were generously provided by the Pediatric Preclinical Testing Consortium (PPTC), previously called the Pediatric Preclinical Testing Program (PPTP). These lines are maintained by serial passage in severe combined immune deficient (SCID) mice as described previously (31).

**Antibodies and reagents:** Primary antibodies against STMN1, phospho-STMN1 (S38), sirtuin 1 (SIRT1),  $\beta$ -tubulin,  $\beta$ III-tubulin, specificity protein 1 (Sp1), cyclin D1, p27, poly ADP ribose polymerase (PARP), microtubule-associated protein light chain 3-II (LC3-II), GAPDH and horseradish peroxidase (HRP)-conjugated secondary antibodies were purchased from Cell Signaling Technology (Danvers, MA). For immunofluorescence, Alexa 488-labeled secondary antibodies were from Jackson ImmunoResearch Laboratories (West Grove, PA). Gemcitabine was purchased from Selleckchem (Houston, TX). Eribulin was obtained from the Pharmacy, Alfred I duPont Hospital for Children.

**RT-qPCR and PCR:** Total RNA was isolated from cells and tumors using Trizol reagent (Invitrogen, Carlsbad, CA). First strand cDNA was synthesized with the High Capacity cDNA Synthesis Kit (Applied Biosystems, Foster City, CA). TaqMan miRNA gene expression assays for human miR-34a and miR-361 (internal reference) were purchased from Applied Biosystems. Gene amplification was performed using the 7900HT Fast Real-Time PCR system (Applied Biosystems). The primer sets were STMN1: F - 5' TTCCCTGGAGGAAATTCAGA 3' and R - 5' TCTCGTGCTCTCGTTTCTCA 3'; TUBB2: F - 5'

AAATATGTACCTCGGGCCATC 3' and R – 5' GTTATTCCCGGCTCCACTCT 3'; TUBB3: F – 5' GCAACTACGTGGGCGACT 3' and R – 5' CGAGGCACGTA CT TGTGAGA 3'; E2F3: F – 5' GCAGCCTCCTCTACACCAC 3' and 5' – AGGTACTGATGACCGCTTTCT - 3' and GAPDH: F - 5' TGCACCACCAACTGCTTAGC 3' and R - 5' GGCATGGACTGTGGTCATGAG 3'. cDNA loading was normalized to GAPDH and gene expression was determined using the  $\Delta\Delta\text{Ct}$  method of relative quantification. Data are presented as mean  $\pm$  SE of three measurements.

**Transfections with lipofectamine (for miRNA and siRNA oligonucleotides):** SaOS and 143B cells were seeded into 6-well plates ( $2.5 \times 10^5$  cells/well) in medium without antibiotics. After 24 hours, each cell line was transiently transfected with either precursor hsa-miR-34a-5p (miR-34a) (ThermoFisher Scientific, Carlsbad, CA) or the non targeting miRNA control (miR-C) using RNAi max lipofectamine (Invitrogen, Carlsbad, CA) according to the manufacture's protocol. SMARTpool siRNA oligonucleotides targeting STMN1, Sp1, and a non-targeting control, purchased from Dharmacon (Lafayette, CO). After 6 hours, the cells were grown in medium supplemented with 10% FBS and antibiotics. Cells were harvested for analysis 48 hours after transfections.

**Transfections with Nucleofector (for plasmid DNA):** Human STMN1 (transcript variant 1) expression plasmid was purchased from Origen (Rockville, MD). OS cells were transfected with STMN1 plasmid using the Amaxa nucleofector transfection reagent (Lonza, Allendale NJ) according to manufacturer's protocol.

**Cell viability assay:** SaOS and 143B cells were seeded into 96-well plates ( $2 \times 10^3$  cells/well) in medium without antibiotics and grown for 24 hours. Cells were transfected with miRNAs for 72 hours, siRNAs for 48 hours or treated with eribulin or gemcitabine for 24 hours. Viable cells were measured using the Cell Titer Blue assay (Promega, Madison WI) according to manufacturer's protocol. Absorbance values were read at 570nm using a Victor4 plate reader (Perkin Elmer, Waltham, MA). Data is represented as the mean of six measurements  $\pm$  SE.

**miRNA Biotin pulldown:** Biotin labeled miR-34a (bi-miR-34a) was synthesized by Dharmacon (Lafayette, CO). Bi-miR-34a or biotin labeled cel-miR-67 (bi-miR-C) control molecules were transfected into SaOS and 143B cells using RNAi max lipofectamine (Invitrogen). After 24 hours, cells were incubated with lysis buffer [50 mM Tris-HCl (pH 7.5), 300 mM KCl, 12 mM MgCl<sub>2</sub>, 1% NP-40, 1 mM DTT] supplemented with complete protease inhibitor-EDTA free (Roche), RNase inhibitor (Promega, 200 U/ml), ribonucleoside-vanadyl complex (Sigma-Aldrich, St. Louis, MO). Bi-miR-34a and mRNA complexes were captured with Streptavidin-Dynabeads coated magnetic beads (Invitrogen) by incubation for 4 hours. Beads were washed 5x [10 mM Tris-HCl (pH 7.5), 3 mM MgCl<sub>2</sub>, 14 mM NaCl, 1 mM DTT and 5% glycerol] and bound mRNA was purified using Trizol (Invitrogen) and analyzed by PCR using forward and reverse primers against *STMN1*, *TUBB3* (negative control) and *E2F3* (positive control). Non-specific binding of RNA to the magnetic beads was analyzed using bi-miR-C.

**Luciferase assay:** The pMiRTarget plasmid containing the *STMN1* mRNA 3'UTR sequence fused to the luciferase reporter gene was constructed by Origene (Rockville, MD). SaOS and 143B cells were co-transfected with pMiRTarget *STMN1* 3'UTR and either pre-miR-34a or non-targeting control miR-C oligonucleotides with Lipofectamine 3000 (Invitrogen). After 24 hours, cell extracts were prepared and reporter gene activity was determined using the Dual-Luciferase Reporter Assay (Promega, Madison, WI) according to manufacturer's protocol. The Victor plate reader was used to measure luciferase reporter units (PerkinElmer, Waltham, MA). Luciferase measurements were normalized to *Renilla luciferase* used as the internal control.

**Immunoblot:** Cells were treated with miR-34a, or siRNA, or microtubule targeting agents (MTAs) as single agents or in combination and harvested at time points specified. Cells were lysed in RIPA buffer (Invitrogen) supplemented with protease and phosphatase inhibitors (ThermoFisher Scientific), lysates were pre-cleared by centrifugation and protein concentration was determined (Pierce, CA). Proteins were separated by SDS-PAGE, transferred to nitrocellulose membranes, incubated with primary antibodies, horseradish peroxidase-conjugated secondary antibodies and subjected to ECL analysis (GE Healthcare, Pittsburgh, PA).



**Immunofluorescence staining and confocal microscopy:** Poly-L-lysine coated glass coverslips were placed in 12-well plates and overlaid with  $2 \times 10^3$  SaOS and 143B cells. The cells were grown overnight, then transfected with miR-34a before processing for immunofluorescence. Cells were fixed with formaldehyde for 20 min at room temperature, and rehydrated with PBS containing  $\text{CaCl}_2$  (0.1 mM),  $\text{MgCl}_2$  (1 mM) and 0.2% BSA. Subsequently, the cells were incubated with the primary antibodies (1:200 dilution) followed by secondary antibodies (1:200). Hoechst dye (Thermo Fisher Scientific) was used for nuclear staining at 1:10,000. Fluorescence images were captured using a Leica TCS SP5 scanning confocal microscope (Leica Microsystems Inc., Buffalo Grove, IL) with the 63 $\times$  oil objective lens. Images were processed using Photoshop (Adobe Systems Inc., San Jose, CA).

**Cell Cycle Analysis:** SaOS and 143B cells ( $2 \times 10^5$ ) were transfected with miR-34a for 72 hours and subjected to propidium iodide (PI) staining (Sigma). Briefly, cells were trypsinized, washed with PBS and fixed with 70% ethanol for 30 mins at  $-20^\circ \text{C}$ . Cells were washed, pelleted and resuspended in 500  $\mu\text{l}$  of PI/RNase solution for 15 min at room temperature. Cell cycle analysis was performed using the NovoCyte flow cytometer (ACEA Biosciences, San Diego, CA).

**Statistical Analysis:** The relationship between the miRNA and mRNA targets was tested with Pearson's correlation coefficient. Synergy of miR-34a and drug combination therapies was quantified using the CompuSyn software (ComboSyn, Inc., Paramus, NJ.) to calculate the combination index (CI) based on the Chou-Talalay method (32) where  $\text{CI} < 1$ ,  $\text{CI} = 1$ , and  $\text{CI} > 1$  indicate synergistic, additive, and antagonistic effects, respectively. All statistical analyses used the two-tailed unpaired Student t-test and were calculated using GraphPad Prism software (GraphPad Software Inc., La Jolla CA). Data was expressed as mean value  $\pm$  SE (standard error). Statistical significance was defined as  $p < 0.05$  and is denoted by asterisks in the figures.

## RESULTS

### 1. **Endogenous expression of miR-34a correlates inversely with *STMN1* mRNA expression in OS cell lines and xenograft tumors.**

Expression of miR-34a was evaluated by reverse transcriptase-quantitative PCR (RT-qPCR) in 5 human OS cell lines (SaOS, 143B, HOS, U2OS, MG-63) and 9 tumors of the PPTC OS xenograft panel (OS1, OS2, OS9, OS17, OS31 OS33, OS46, OS51 OS56). In agreement with earlier reports (15), all OS specimens demonstrated attenuated levels of miR-34a (Figure 1A), relative to human osteoblasts (CRL11372). Bioinformatics ([www.microRNA.org](http://www.microRNA.org)) was used to predict candidate genes that are potentially regulated by miR-34a and *STMN1* was identified as a novel target that has not been studied. The *STMN1* protein regulates microtubule dynamics and high expression correlates with tumor progression in OS (25). The alignment predicted between the miR-34a seed sequence and the *STMN1* 3'UTR recognition sequence is shown in Figure 1A. RT-qPCR analysis of *STMN1* mRNA levels in the OS cell lines and xenograft tumors showed high *STMN1* expression, in comparison with osteoblasts, Figure 1A. Pearson correlation analysis revealed that levels of *STMN1* were negatively correlated with miR-34a ( $r=-0.35$ ,  $p<0.05$ ), Figure 1B. To confirm this finding, SaOS, 143B, HOS and U2OS cell lines were transfected with miR-34a precursors. Overexpression of miR-34a relative to control cells transfected with miR-C (Figure S1) significantly reduced *STMN1* mRNA levels in SaOS and 143B cells (by 0.12-fold and 0.52-fold, respectively,  $p<0.05$ ), Figure 1C. In addition, immunoblot analysis demonstrated *STMN1* protein levels were downregulated in miR-34a expressing cells (Figure 1D). Taken together, these results imply that miR-34a is involved in the regulation of *STMN1* in OS.

### 2. **miR-34a targets the *STMN1* mRNA 3'UTR in vitro.**

The biotin pulldown assay was used to assess target interactions between miR-34a and *STMN1* mRNA. SaOS and 143B cells transfected with either bi-miR-34a or bi-miR-C controls were treated with streptavidin beads. Bound mRNA was isolated and subjected to PCR analysis. Using *STMN1* specific primers, amplification of *STMN1* in cells expressing bi-miR-34a, but not those with bi-miR-C (Figure 2A) was observed, validating *STMN1* as a direct miR-34a target gene *in vitro*. There was no amplification of the non-targeted *TUBB3* gene (negative control), while *E2F3*, a known miR-34a target (13) was detected (positive control), Figure 2A. We examined the specific interaction site of miR-34a on the *STMN1* 3'UTR using the luciferase reporter assay. Co-

transfection of SaOS and 143B cells with the pMiRTarget plasmid, containing the *STMN1* 3'UTR sequence inserted downstream from the firefly luciferase gene, was performed with either miR-34a or miR-C. Red fluorescence protein was used as a reporter to monitor transfection efficiency and both cell lines were >80% efficiency. OS cells expressing miR-34a showed significantly lower luciferase activity in comparison to controls (Figure 2B). These results confirmed that miR-34a binds the recognition sequence of *STMN1* mRNA within the 3'UTR. In addition, cell viability measurements demonstrated that the restoration of miR-34a reduced the percentage of viable SaOS cells by 37.1%, and of 143B by 38.9% after 72 hours ( $p < 0.05$ ), Figure 2C. Collectively, our data demonstrate that miR-34a binds *STMN1* mRNA at the 3'UTR and induces growth inhibition *in vitro* in OS cells.

### **3. *In vitro* disruption of miR-34a on tubulin and the microtubule network.**

The *STMN1* protein binds and sequesters  $\beta$ -tubulin monomers to destabilize microtubules and prevent mitotic spindle assembly (19). This suggests that microtubule stability could be affected by the observed effects of miR-34a on *STMN1*. Levels of class II and III  $\beta$ -tubulin isotypes were analyzed in OS cells transfected with miR-34a. Overexpression of miR-34a did not affect the expression of *TUBB2A* (encoding  $\beta$ II-tubulin), data not shown. In contrast, levels of *TUBB3* (encoding  $\beta$ III-tubulin) were significantly higher, relative to miR-C controls, Figure 3A. The increase in gene expression correlated with increased  $\beta$ III-tubulin protein levels (Figure 3B, top panel). We also determined whether siRNA-mediated *STMN1* inhibition alters  $\beta$ -tubulin expression. Immunoblot analysis confirmed that *STMN1* knockdown was >70% and >90% efficiency for SaOS and 143B, respectively (Figure 3B, lower panel). Notably, direct silencing of *STMN1* increased protein levels of  $\beta$ III-tubulin but there was no effect on total  $\beta$ -tubulin protein (Figure 3B, lower panel). Immunofluorescence staining and confocal imaging of OS cells using antibodies against *STMN1* and  $\beta$ III-tubulin were analyzed. Representative images shown for the 143B cell line (Figure 3C) demonstrate that *STMN1* protein, which is distributed throughout the cytoplasm in control cells (top panels i-iii), was lower in miR-34a expressing cells (top panels, iv-vi). Inducible  $\beta$ III-tubulin expression was observed (bottom panels, iii-vi), confirming immunoblot results. Further, miR-34a expressing cells demonstrated reduced polymerized tubulin, in comparison to untreated controls, Figure 3D, panels iv, v and vi. Similar disruption of the microtubule skeleton was observed in cells subjected to siRNA-mediated *STMN1* knockdown (Figure 3D, panels vii, viii and ix). Thus, miR-34a disrupts

the microtubule network and acts through the inhibition of STMN1 and increased expression of  $\beta$ III-tubulin *in vitro* in OS.

#### **4. *miR-34a mediates cell cycle arrest, autophagy and apoptosis through the regulation of STMN1.***

Next we investigated putative downstream effectors of miR-34a. Consensus binding sequences for the Sp1 transcription factor are contained within the  $\beta$ III-tubulin promoter (33), but the molecular mechanisms regulating transcription of  $\beta$ III-tubulin are not clear. Immunoblot analysis revealed that siRNA silencing of Sp1 in SaOS, 143B, HOS and U2OS upregulated  $\beta$ III-tubulin protein (Figure 4A, Lane 4), indicating that Sp1 negatively regulates  $\beta$ III-tubulin expression. Comparative increases in levels of  $\beta$ III-tubulin protein in miR-34a expressing cells (Figure 4A, Lane 3) suggests Sp1 may be an indirect downstream effector of miR-34a that is involved in the regulation of  $\beta$ III-tubulin. We determined the effect of miR-34a on the cell cycle distribution in SaOS and 143B cells transfected with miR-34a, followed by STMN1 overexpression, using a STMN1 expression plasmid (Figure 4B). Our data revealed that treatment with miR-34a only, led to cell cycle arrest in G1 and G2/M phase, and apoptosis (sub G1), Figure 4B, panel ii and Table 1. Restoration of STMN1 reduced the number of miR-34a expressing cells in G1 and G2/M (Figure 4B, panel iii). Notably, cell cycle markers cyclin D1 and p27 were upregulated in miR-34a expressing cells (Figure 4C), to confirm both G1 and G2-phase arrest occurred in these cells. Similar upregulation in levels of cyclin D1 and p27 were observed in HOS and U2OS (Figure S2). In addition, decreases in both proteins were evident when STMN1 was restored. Protein expression of cleaved PARP was also higher, confirming that miR-34a induced apoptosis (Figure 4C). Immunofluorescence images (Figure 4D) illustrate that cells transfected with miR-34a expressed high levels of LC3 I/II protein. These cells show morphological changes (rounded) and aberrant nuclei (enlarged and multinucleated) that are in line with cellular alterations associated with cell death response to miR-34a (Figure 3C and 3D). Taken together, these data demonstrate that miR-34a triggers autophagy and cell death *in vitro* in OS.

#### **5. *Combining miR-34a with microtubule inhibitors and chemotherapy enhances cytotoxicity in vitro in OS cells.***

Based on the ability of miR-34a to regulate key components in the microtubule network, we analyzed the effects of miR-34a with eribulin and gemcitabine, on OS cell growth. SaOS and 143B cells were treated with

multiple combinations of both agents (miR-34a/eribulin or miR-34a/gemcitabine) and cell viability was assayed to determine effect levels (fraction affected, Fa) and combination index (CI) values. Drug interactions were classed as additive (CI=1), antagonistic (CI>1), or synergistic (CI<1). Results presented in Figure 5A and Table 2 show combination therapies consisting of miR-34a/eribulin or miR-34a/gemcitabine were synergistic for OS cell lines. Interestingly, immunoblot analysis of STMN1 protein revealed increases in levels of phosphorylated STMN1 by eribulin treatment, in both cell lines, Figure 5B. STMN1 phosphorylation is associated with formation of the mitotic spindle and microtubule stabilization and is implicated in resistance mechanisms to MTAs (34). Importantly, the expression of STMN1 protein and consequently STMN1 phosphorylation, were abrogated when the two agents were combined. Representative immunostaining and confocal imaging for 143B cells using antibodies against STMN1 confirmed that eribulin did not affect STMN1 protein levels (Figure 5C, panels iv-vi) in comparison to untreated cells (panels i-iii), while co-treatment with miR-34a and eribulin showed substantial downregulation of STMN1 (panels vii-ix). Immunoblots (Figure 5B) also show that protein levels of  $\beta$ III-tubulin, cleaved PARP and LC3-I/II were higher in the combination group, in comparison to the single-agent eribulin. Taken together, this suggests that combining miR-34a and eribulin achieves synergistic interactions through STMN1 inhibition. A schematic summarizing the activity of miR-34a in modulating the microtubule network in OS is presented in Figure 5D. Overall, our data present a novel mechanism of action of miR-34a in regulating STMN1 and microtubule stability and provides a compelling model for the involvement of miR-34a in augmenting the antitumor activity of MTAs in OS.

## DISCUSSION

The survival of pediatric patients with metastatic and recurrent OS has not improved over the past 20 years due in part, to the fact that few new therapies are effective in these patients. Rigorous preclinical studies are identifying novel agents and treatment strategies that may lead to the development of new clinical trials to improve survival outcomes. miR-34a has emerged as a promising agent for the management and therapy of liver cancer and is the first miRNA-based cancer therapy that was tested in clinical trials (35). The antitumor activity of miR-34a has been demonstrated *in vitro* and *in vivo* in OS (15) but the molecular mechanism of action is not well characterized. Our current findings identify miR-34a as a critical molecule that controls microtubule stability and growth of OS cells, and add to the rationale for clinical investigation of miR-34a as a therapeutic agent.

In this study, human OS cell lines and pediatric OS xenograft tumors were used to confirm previous reports of low levels of miR-34a in OS (15, 36). Previous studies have demonstrated the function of miR-34a as a tumor suppressor in the control of cell cycle progression, cell proliferation, migration and survival in cancer, including OS (13, 15). Our findings are consistent with these functions of miR-34a, and reveal that microtubule destabilization is a key event in the anti-tumor activity. The validation of STMN1 as a miR-34a target gene attributes a novel role to miR-34a in the regulation of microtubule stability. Relative to normal osteoblasts, miR34a and STMN1 mRNA were inversely correlated in OS cells and xenograft tumors and inhibition of the STMN1 oncogene by the restoration of miR-34a, supports the tumor-suppressing characteristics of miR-34a.

STMN1 is highly expressed in several types of cancer (22, 23), as well as OS (21, 25), and this correlates with poor prognosis and resistance to chemotherapy agents. Restoration of downregulated miR-34a significantly reduced STMN1 gene and protein expression and arrested the growth of OS cells, suggesting the antitumor activity of miR-34a in OS is mediated through the microtubule network. The sensitivity of OS cells that lack endogenous p53, and that express wild-type p53, demonstrated that the p53 status is not a prevailing indicator of miR-34a activity, as the general responses to miR-34a restoration were similar for all cell lines. This is in line with emerging studies that suggest that endogenous p53 is not a prerequisite for miR-34a tumor suppressor activity and miR-34a is capable of inhibition in p53-null and p53-expressing cancer cell lines (37).

Evidence supporting the oncogenic role of STMN1 in OS can be inferred from experiments demonstrating high levels of expression in OS tumors (21, 25), the cytogenetic location to 1p36, a known cancer-related region in OS (11, 12), and the role in growth regulation (34, 38). Attenuation of STMN1 suppresses growth of STMN1 expressing OS cells (33, 36), indicating elevated levels of STMN1 play an important role in disease progression. Selective strategies to inhibit cell division through the silencing of STMN1 have been studied using ribozymes (38), siRNA targeting (34) and miRNAs (28, 29). The therapeutic inhibition of STMN1 using a bi-functional shRNA plasmid (pbi-shRNA STMN1) that cleaves *STMN1* mRNA was evaluated in melanoma and OS (39) and in patients with superficial advanced refractory cancer (40) and is undergoing further clinical testing. miR-34a mediated inhibition of STMN1 demonstrated a decrease in cell proliferation and the induction of apoptosis in OS cells. The expression of  $\beta$ III-tubulin was upregulated and similar to siRNA-mediated inhibition of STMN1. Notably, depletion of STMN1 promoted loss of microtubule polymerization and destabilization of the microtubule network in vitro in OS.

Sp1 transcription factor modulates the expression of a number of essential oncogenes and tumor suppressors (41). The promoter region for  $\beta$ III-tubulin contains multiple potential binding sequences for Sp1 as well as for activating protein-2 (AP2) and a central nervous system enhancer regulatory element and an E-box (33), but the regulation of  $\beta$ III-tubulin remains largely unknown. Silencing Sp1 with siRNA increased the expression of  $\beta$ III-tubulin and activated apoptosis. These observations imply that the Sp1 transcription factor may be an indirect downstream effector of miR-34a signaling that is involved in the upregulation of  $\beta$ III-tubulin. Further, the miR-34a involvement on Sp1 activity could be mediated through post-translational modifications or other transcriptional co-factors (41). Several reports indicate that the constitutive expression of  $\beta$ III-tubulin is frequently linked to tumor aggressiveness, resistance to chemotherapy, and patient relapse (42-44) and both high STMN1 and  $\beta$ III-tubulin expression are implicated with poor survival in ovarian cancer patients (22). Mechanistically, microtubules that are enriched in heterodimers formed by  $\beta$ III-tubulin are unstable polymers and the overexpression of  $\beta$ III-tubulin increases the rate of microtubule detachment from microtubule organizing centers, and reduces the stability of microtubule networks (45, 46). Our data are in agreement with these studies, as inducible expression of  $\beta$ III-tubulin in response to miR-34a overexpression correlated with microtubule destabilization, cell cycle arrest and apoptosis. In this context, inducible expression of  $\beta$ III-tubulin

cannot be associated with an aggressive phenotype nor linked to resistance and survival. Therefore, while high constitutive  $\beta$ III-tubulin expression could be a marker for aggressive tumors, low constitutive expression and inducible  $\beta$ III-tubulin expression are associated with destabilization of microtubules and OS cell death.

The influence on multiple cellular pathways may also suggest that miR-34a can act synergistically with conventional, cytotoxic therapies. The elevated expression of STMN1 and  $\beta$ III-tubulin may be important in regulating sensitivity to broad classes of chemotherapy drugs. Mechanisms underlying resistance to microtubule inhibitors that occur at the microtubules include mutations, alterations of tubulin isotypes or regulatory proteins (47). In the current study, we have demonstrated that cells that were exposed to eribulin showed higher levels of phosphorylation of STMN1. The phosphorylation of STMN1 disrupts the formation of STMN1-tubulin complexes and increases the availability of free  $\beta$ -tubulin for microtubule assembly, which can confer resistance to MTAs. Combining miR-34a and MTAs confirmed that OS cells expressing STMN1 protein were more sensitive to microtubule inhibition, by STMN1 silencing. In line with these findings, the strategy of combining mir-34a with paclitaxel has been reported to overcome resistance to paclitaxel in hormone-refractory prostate cancer cells (48) and to treat murine melanoma metastasized to the lungs of mice (49). The implication is that in a selective molecular background involving STMN1 deletion, inducible  $\beta$ III-tubulin may enhance the response to these therapies.

This is the first report demonstrating that miR-34a regulates STMN1 and has a modulatory role in microtubule stability. Birnie et al., (50) demonstrate a miR-223/STMN1/tubulin regulated pathway in malignant pleural mesothelioma and suggest a possible conservation of function. Our findings are in line with the anti-tumor signal transductions for miR-34a and support further investigations into combining miR-34a with microtubule inhibitors as a therapeutic strategy. Microtubule inhibitors show limited efficacy in OS patients, and have not been incorporated into standard neoadjuvant therapy regimens or in common retrieval regimens. OS cells and tumors resistant to MTAs may survive in the presence of microtubule inhibition through the cellular efflux of drug, ineffective target interaction and deficiencies in the apoptotic pathway. Several MTAs are in active clinical development in pediatric sarcomas. A recent Children's Oncology Group trial (NCT02097238) failed to clearly demonstrate a role for eribulin in neo-adjuvant chemotherapy for recurrent and refractory OS. As new agents move forward in clinical development, understanding mechanisms of resistance and identifying biomarkers of



response will be imperative. While an association between high levels of STMN1 and  $\beta$ III-tubulin in cancer is not novel (22), our data specifically demonstrate STMN1 inhibition and inducible  $\beta$ III-tubulin in OS could alter microtubule stability. We have also identified STMN1 and  $\beta$ III-tubulin expression as biomarkers of response to therapy.

In conclusion, these mechanistic studies have identified a key role of miR-34a in OS, centered on the regulation of STMN1 and microtubule stability. Our studies demonstrate the feasibility of using miR-34a as a miRNA-based therapy for reducing STMN1 expression *in vitro* in OS to promote microtubule mediated cell death. Our data also show that miR-34a targets cell processes distinct from MTAs, through the coordinated regulation of the miR-34a/STMN1 $\beta$ III-tubulin axis. Ongoing studies aim to elucidate the effect miR-34a can exert on STMN1 and microtubules, in relevant *in vivo* OS preclinical models. Of note, the recent failure of MR34X as a miR-34a replacement therapy for patients with liver cancer, highlights that current miRNA delivery approaches are limited in their safety and efficacy. Comprehensive molecular studies such as this, as well as the development of reliable miRNA delivery systems, and characterization of the adaptive and innate immune response will be crucial to support clinical trials for miR-34a replacement in patients with OS.

**ACKNOWLEDGMENTS:** The authors thank Dr. Richard Gorlick (The Children's Hospital at Montefiore, New York) for providing the PPTC OS xenograft tumors for this study.

## REFERENCES

1. Geller DS, Gorlick R. Osteosarcoma: a review of diagnosis, management, and treatment strategies. *Clin Adv Hematol Oncol*. 2010;8:705-18.
2. Mirabello L, Troisi RJ, Savage SA. Osteosarcoma incidence and survival rates from 1973 to 2004: data from the Surveillance, Epidemiology, and End Results Program. *Cancer*. 2009;115:1531-43.
3. Bielack S, Jurgens H, Jundt G, Kevric M, Kuhne T, Reichardt P, et al. Osteosarcoma: the COSS experience. *Cancer Treat Res*. 2009;152:289-308.
4. Bartel DP. MicroRNAs: genomics, biogenesis, mechanism, and function. *Cell*. 2004;116:281-97.
5. Bertoli G, Cava C, Castiglioni I. MicroRNAs: New Biomarkers for Diagnosis, Prognosis, Therapy Prediction and Therapeutic Tools for Breast Cancer. *Theranostics*. 2015;5:1122-43.
6. Muralidhar GG, Barbolina MV. The miR-200 Family: Versatile Players in Epithelial Ovarian Cancer. *Int J Mol Sci*. 2015;16:16833-47.
7. Ling H, Fabbri M, Calin GA. MicroRNAs and other non-coding RNAs as targets for anticancer drug development. *Nat Rev Drug Discov*. 2013;12:847-65.
8. Heneghan HM, Miller N, Kerin MJ. Circulating miRNA signatures: promising prognostic tools for cancer. *J Clin Oncol*. 2010;28:e573-4; author reply e5-6.
9. Welch C, Chen Y, Stallings RL. MicroRNA-34a functions as a potential tumor suppressor by inducing apoptosis in neuroblastoma cells. *Oncogene*. 2007;26:5017-22.
10. Henrich KO, Schwab M, Westermann F. 1p36 tumor suppression--a matter of dosage? *Cancer Res*. 2012;72:6079-88.
11. Man TK, Lu XY, Jaeweon K, Perlaky L, Harris CP, Shah S, et al. Genome-wide array comparative genomic hybridization analysis reveals distinct amplifications in osteosarcoma. *BMC Cancer*. 2004;4:45.
12. Tesser-Gamba F, Petrilli AS, de Seixas Alves MT, Filho RJ, Juliano Y, Toledo SR. MAPK7 and MAP2K4 as prognostic markers in osteosarcoma. *Hum Pathol*. 2012;43:994-1002.
13. Misso G, Di Martino MT, De Rosa G, Farooqi AA, Lombardi A, Campani V, et al. Mir-34: a new weapon against cancer? *Mol Ther Nucleic Acids*. 2014;3:e194.
14. Nakatani F, Ferracin M, Manara MC, Ventura S, Del Monaco V, Ferrari S, et al. miR-34a predicts survival of Ewing's sarcoma patients and directly influences cell chemo-sensitivity and malignancy. *J Pathol*. 2012;226:796-805.
15. He C, Xiong J, Xu X, Lu W, Liu L, Xiao D, et al. Functional elucidation of MiR-34 in osteosarcoma cells and primary tumor samples. *Biochem Biophys Res Commun*. 2009;388:35-40.
16. Sampson VB, Yoo S, Kumar A, Vetter NS, Kolb EA. MicroRNAs and Potential Targets in Osteosarcoma: Review. *Front Pediatr*. 2015;3:69.
17. Yan K, Gao J, Yang T, Ma Q, Qiu X, Fan Q, et al. MicroRNA-34a inhibits the proliferation and metastasis of osteosarcoma cells both in vitro and in vivo. *PLoS One*. 2012;7:e33778.
18. Tarasov V, Jung P, Verdoodt B, Lodygin D, Epanchintsev A, Menssen A, et al. Differential regulation of microRNAs by p53 revealed by massively parallel sequencing: miR-34a is a p53 target that induces apoptosis and G1-arrest. *Cell Cycle*. 2007;6:1586-93.
19. Ringhoff DN, Cassimeris L. Stathmin regulates centrosomal nucleation of microtubules and tubulin dimer/polymer partitioning. *Mol Biol Cell*. 2009;20:3451-8.
20. Gavet O, Ozon S, Manceau V, Lawler S, Curmi P, Sobel A. The stathmin phosphoprotein family: intracellular localization and effects on the microtubule network. *J Cell Sci*. 1998;111 ( Pt 22):3333-46.
21. Kumar R, Haugen JD. Human and rat osteoblast-like cells express stathmin, a growth-regulatory protein. *Biochem Biophys Res Commun*. 1994;201:861-5.
22. Su D, Smith SM, Preti M, Schwartz P, Rutherford TJ, Menato G, et al. Stathmin and tubulin expression and survival of ovarian cancer patients receiving platinum treatment with and without paclitaxel. *Cancer*. 2009;115:2453-63.
23. Jeon TY, Han ME, Lee YW, Lee YS, Kim GH, Song GA, et al. Overexpression of stathmin1 in the diffuse type of gastric cancer and its roles in proliferation and migration of gastric cancer cells. *Br J Cancer*. 2010;102:710-8.

24. Machado-Neto JA, de Melo Campos P, Favaro P, Lazarini M, Lorand-Metze I, Costa FF, et al. Stathmin 1 is involved in the highly proliferative phenotype of high-risk myelodysplastic syndromes and acute leukemia cells. *Leuk Res.* 2014;38:251-7.
25. Wang R, Dong K, Lin F, Wang X, Gao P, Wei SH, et al. Inhibiting proliferation and enhancing chemosensitivity to taxanes in osteosarcoma cells by RNA interference-mediated downregulation of stathmin expression. *Mol Med.* 2007;13:567-75.
26. Carney BK, Caruso Silva V, Cassimeris L. The microtubule cytoskeleton is required for a G2 cell cycle delay in cancer cells lacking stathmin and p53. *Cytoskeleton (Hoboken).* 2012;69:278-89.
27. Byrne FL, Yang L, Phillips PA, Hansford LM, Fletcher JI, Ormandy CJ, et al. RNAi-mediated stathmin suppression reduces lung metastasis in an orthotopic neuroblastoma mouse model. *Oncogene.* 2014;33:882-90.
28. Li X, Yao R, Yue L, Qiu W, Qi W, Liu S, et al. FOXM1 mediates resistance to docetaxel in gastric cancer via up-regulating Stathmin. *J Cell Mol Med.* 2014;18:811-23.
29. Hassan MK, Watari H, Mitamura T, Mohamed Z, El-Khamisy SF, Ohba Y, et al. P18/Stathmin1 is regulated by miR-31 in ovarian cancer in response to taxane. *Oncoscience.* 2015;2:294-308.
30. Sun Q, Liu T, Zhang T, Du S, Xie GX, Lin X, et al. MiR-101 sensitizes human nasopharyngeal carcinoma cells to radiation by targeting stathmin 1. *Mol Med Rep.* 2015;11:3330-6.
31. Houghton PJ, Morton CL, Tucker C, Payne D, Favours E, Cole C, et al. The pediatric preclinical testing program: description of models and early testing results. *Pediatr Blood Cancer.* 2007;49:928-40.
32. TC. C. Drug combination studies and their synergy quantification using the Chou-Talalay method. *Cancer Res.* 2010;70:7.
33. Dennis K, Uittenbogaard M, Chiramello A, Moody SA. Cloning and characterization of the 5'-flanking region of the rat neuron-specific Class III beta-tubulin gene. *Gene.* 2002;294:269-77.
34. Alli E, Yang JM, Ford JM, Hait WN. Reversal of stathmin-mediated resistance to paclitaxel and vinblastine in human breast carcinoma cells. *Mol Pharmacol.* 2007;71:1233-40.
35. Agostini M, Knight RA. miR-34: from bench to bedside. *Oncotarget.* 2014;5:872-81.
36. Wang Y, Jia LS, Yuan W, Wu Z, Wang HB, Xu T, et al. Low miR-34a and miR-192 are associated with unfavorable prognosis in patients suffering from osteosarcoma. *Am J Transl Res.* 2015;7:111-9.
37. Christoffersen NR, Shalgi R, Frankel LB, Leucci E, Lees M, Klausen M, et al. p53-independent upregulation of miR-34a during oncogene-induced senescence represses MYC. *Cell Death Differ.* 2009;17:236-45.
38. Mistry SJ, Benham CJ, Atweh GF. Development of ribozymes that target stathmin, a major regulator of the mitotic spindle. *Antisense Nucleic Acid Drug Dev.* 2001;11:41-9.
39. Phadke AP, Jay CM, Wang Z, Chen S, Liu S, Haddock C, et al. In vivo safety and antitumor efficacy of bifunctional small hairpin RNAs specific for the human Stathmin 1 oncoprotein. *DNA Cell Biol.* 2011;30:715-26.
40. Barve M, Wang Z, Kumar P, Jay CM, Luo X, Bedell C, et al. Phase 1 Trial of Bi-shRNA STMN1 BIV in Refractory Cancer. *Mol Ther.* 2015;23:1123-30.
41. Safe S, Abdelrahim M. Sp transcription factor family and its role in cancer. *Eur J Cancer.* 2005;41:2438-48.
42. Urano N, Fujiwara Y, Doki Y, Kim SJ, Miyoshi Y, Noguchi S, et al. Clinical significance of class III beta-tubulin expression and its predictive value for resistance to docetaxel-based chemotherapy in gastric cancer. *Int J Oncol.* 2006;28:375-81.
43. Paradiso A, Mangia A, Chiriatti A, Tommasi S, Zito A, Latorre A, et al. Biomarkers predictive for clinical efficacy of taxol-based chemotherapy in advanced breast cancer. *Ann Oncol.* 2005;16 Suppl 4:iv14-9.
44. Seve P, Lai R, Ding K, Winton T, Butts C, Mackey J, et al. Class III beta-tubulin expression and benefit from adjuvant cisplatin/vinorelbine chemotherapy in operable non-small cell lung cancer: analysis of NCIC JBR.10. *Clin Cancer Res.* 2007;13:994-9.
45. Ganguly A, Yang H, Cabral F. Class III beta-tubulin counteracts the ability of paclitaxel to inhibit cell migration. *Oncotarget.* 2011;2:368-77.
46. Hari M, Yang H, Zeng C, Canizales M, Cabral F. Expression of class III beta-tubulin reduces microtubule assembly and confers resistance to paclitaxel. *Cell Motil Cytoskeleton.* 2003;56:45-56.
47. Berrieman HK, Lind MJ, Cawkwell L. Do beta-tubulin mutations have a role in resistance to chemotherapy? *Lancet Oncol.* 2004;5:158-64.

48. Kojima K, Fujita Y, Nozawa Y, Deguchi T, Ito M. MiR-34a attenuates paclitaxel-resistance of hormone-refractory prostate cancer PC3 cells through direct and indirect mechanisms. *Prostate*. 2010;70:1501-12.
49. Shi S, Han L, Deng L, Zhang Y, Shen H, Gong T, et al. Dual drugs (microRNA-34a and paclitaxel)-loaded functional solid lipid nanoparticles for synergistic cancer cell suppression. *J Control Release*. 2014;194:228-37.
50. Birnie KA, Yip YY, Ng DCH, Kirschner MB, Reid G, Prêle CM, et al. Loss of miR-223 and JNK Signaling Contribute to Elevated Stathmin in Malignant Pleural Mesothelioma. *Mol Can Res*. 2015;13:13.

## FIGURE LEGENDS:

### Figure 1: Gene expression of endogenous miR-34a and STMN1 for OS cell lines and OS xenografts.

**(A)** Top – Schematic of the alignment between the miR-34a seed sequence and the target recognition sequence of *STMN1* mRNA 3'UTR, predicted by microRNA.org. Bottom - Expression of miR-34a and *STMN1* mRNA in OS cell lines (n=5) and xenografts (n=9) was measured by RT-qPCR and expressed relative to normal osteoblasts. Values are mean of three measurements. **(B)** The correlation between miR-34a expression in OS cells and xenografts and *STMN1* mRNA was analyzed by Pearson's correlation coefficient. **(C)** SaOS and 143B cells were transfected with non-targeting miR-C (control) oligonucleotides or miR-34a precursors and *STMN1* mRNA was measured by RT-qPCR. Results are represented as fold-change relative to miR-C. Graph depicts mean  $\pm$  SE of one representation of three independent experiments. \* denotes  $p < 0.05$ . **(D)** *STMN1* protein expression in untreated, miR-C and miR-34a transfected SaOS, 143B, HOS and U2OS cells was measured by immunoblot. GAPDH was loading control. Representative results of three analyses are shown.

**Figure 2: *In vitro* validation of miR-34a and *STMN1* mRNA association in OS cells.** **(A)** Transcripts that were bound to biotin labeled miR-34a (bi-miR-34a) in miR-34a expressing SaOS and 143B cells were precipitated and analyzed by PCR. DNA gel shows amplification of *STMN* and *E2F3* (positive control) using gene specific primers. *TUBB3* was the negative control. **(B)** Luciferase activity was measured in SaOS and 143B cells co-transfection with pMiRTarget plasmid containing the *STMN1* 3'UTR sequence and miR-34a or miR-C, using the dual-luciferase reporter assay. Values were normalized to *Renilla luciferase* as the internal control. Results are represented as fold-change relative to miR-C. Graph depicts mean  $\pm$  SE of one representation of three independent experiments. \* denotes  $p < 0.05$ . **(C)** Cell viability of SaOS and 143B cells transfected with miR-C or miR-34a was evaluated after 72 hours by the cell titer blue assay. Graphs show the percentage of viable cells for each treatment group. Values represent the mean  $\pm$  SE of six measurements. \* denotes  $p < 0.05$ .

**Figure 3: miR-34a upregulates  $\beta$ III-tubulin and destabilizes microtubules *in vitro* in OS cells.** **(A)** Expression of *TUBB3* in miR-34a expressing SaOS and 143B cells was measured by RT-qPCR. Data is shown relative to miR-C controls. Expression of *TUBB3* is normalized to *GAPDH*. Values are expressed as

mean  $\pm$  SE of triplicate measurements and are representative of two separate experiments. \* denotes  $p < 0.05$ .

**(B)** SaOS and 143B cells were transfected with either miR-34a (top panels) or with siRNA targeting STMN1 (bottom panels) and STMN1,  $\beta$ -tubulin and  $\beta$ III-tubulin protein expression were determined by immunoblot. GAPDH was loading control. Representative results of three analyses are shown. **(C)** Confocal microscopy images for 143B cells transfected with miR-34a for 48 hours and immunostained for STMN1 (orange) and  $\beta$ III-tubulin (green). **(D)** Confocal microscopy images for SaOS and 143B cells transfected with miR-34a (panels iv, v and vi) and siRNA-STMN1 (panels vii, viii and ix) for 72 hours and immunostained for total  $\beta$ -tubulin (green). Cells were counterstained with Hoechst (blue) to visualize nuclei. Scale bars are 25  $\mu$ m.

**Figure 4: miR-34a represses STMN1 and induces cell cycle arrest, apoptosis and autophagy.** **(A)** SaOS, 143B, HOS and U2OS were transfected with either miR-34a or with siRNA targeting Sp1 (bottom panels) and STMN1 and  $\beta$ III-tubulin protein expression were measured by immunoblot. GAPDH was loading control. Representative results of three analyses are shown. **(B)** 143B cells were transfected with miR-34a or an STMN1 expression plasmid. Immunoblot for STMN1 protein (left) is indicated. Cell cycle distribution analysis for untreated, miR-34a-expressing or STMN1 overexpressing 143B cells was assessed by PI staining and flow cytometry analysis. Arrow indicates apoptotic cells. **(C)** Immunoblot analysis of cell cycle markers (cyclin D1 and p27) and apoptotic marker (cleaved PARP) in miR-34a-expressing and STMN1 overexpressing OS cells. GAPDH was loading control. Representative results of three immunoblot analyses are shown. **(D)** Confocal microscopy images for 143B cells transfected with miR-34a for 48 hours and immunostained for LC3 I/II (red) and  $\beta$ III-tubulin (green). Cells were counterstained with Hoechst (blue) to visualize nuclei. Scale bars are 25  $\mu$ m.

**Figure 5: Effect of combining miR-34a with microtubule inhibitors and chemotherapy on cell growth.** **(A)** Chou-Talalay analysis of synergy in SaOS and 143B cell lines using various combinations of miR-34a and eribulin or gemcitabine (Table 1). Cell viability was determined by the cell titer blue method. Values below a combination index = 1 suggest synergy. **(B)** OS cells were treated as indicated and protein expression of  $\beta$ III-tubulin, ph-STMN1, STMN1, cleaved PARP and LC3 I/II in cell lysates was analyzed from each treatment group. GAPDH was loading control. Representative results of three immunoblot analyses are shown. **(C)** Confocal microscopy images for 143B cells treated with eribulin (iv–vi) or co-treated with miR-34a and eribulin

(vii-ix) for 48 hours and immunostained for STMN1 (orange). Cells were counterstained with Hoechst (blue) to visualize nuclei. Scale bars are 25  $\mu$ m. **(D)** A schematic representation of the miR-34a/STMN1/ $\beta$ III-tubulin axis in OS. miR-34a directly binds *STMN1* mRNA to promote transcriptional degradation and translational repression. This upregulates  $\beta$ III-tubulin protein expression and leads to the disruption of the microtubule cytoskeleton, cell cycle arrest and apoptosis. Solid arrows are direct interactions, dotted arrows are indirect interactions. UTR- untranslated region.

**Table 1:** Effect of miR-34a on the cell cycle distribution in SaOS cell line.

	% of SaOS cells		
	G1	S	G2/M
Untreated	33.5	38.15	10.14
miR-34a	38.5	13.64	31.56
miR-34a_ STMN1	42.2	17.9	20.6



**Table 2:** Dose concentrations and Combination Index values.

miR-34a + Eribulin - SaOS				miR-34a + Eribulin – 143B			
miR-34a (nM)	Eribulin (nM)	Fa	CI	miR-34a (nM)	Eribulin (nM)	Fa	CI
0.02	0.002	0.50	0.18	0.2	0.15	0.70	0.21
0.02	0.02	0.56	0.73	0.2	0.4	0.55	0.23
0.02	0.09	0.55	0.80	0.2	0.82	0.27	0.09
0.02	1.0	0.28	0.07	0.2	2.41	0.13	0.09
0.02	10	0.21	0.22	0.2	7.08	0.19	0.45
0.002	0.09	0.51	0.12	0.01	0.82	0.41	0.22
0.2	0.09	0.48	0.91	0.1	0.82	0.18	0.05
1	0.09	0.32	0.06	1	0.82	0.14	0.03
20	0.09	0.29	0.52	20	0.82	0.07	0.01

miR-34a + Gemcitabine - SaOS				miR-34a + Gemcitabine – 143B			
miR-34a (nM)	Gemcitabine (nM)	Fa	CI	miR-34a (nM)	Gemcitabine (nM)	Fa	CI
0.02	0.02	0.48	0.1	0.2	0.14	0.46	0.11
0.02	0.24	0.55	0.58	0.2	0.30	0.51	0.29
0.02	1.2	0.52	0.38	0.2	0.50	0.18	0.11
0.02	14	0.58	>2.0	0.2	1.10	0.21	0.29
0.02	100	0.44	>2.0	0.2	2.44	0.23	0.70
0.002	1.16	0.55	0.21	0.01	0.50	0.41	0.33
0.2	1.16	0.43	0.32	0.1	0.50	0.26	0.17
1	1.16	0.37	0.25	1	0.50	0.19	0.17
20	1.16	0.41	>2.0	20	0.50	0.16	0.10

Fa – Fraction affected; CI – Combination Index

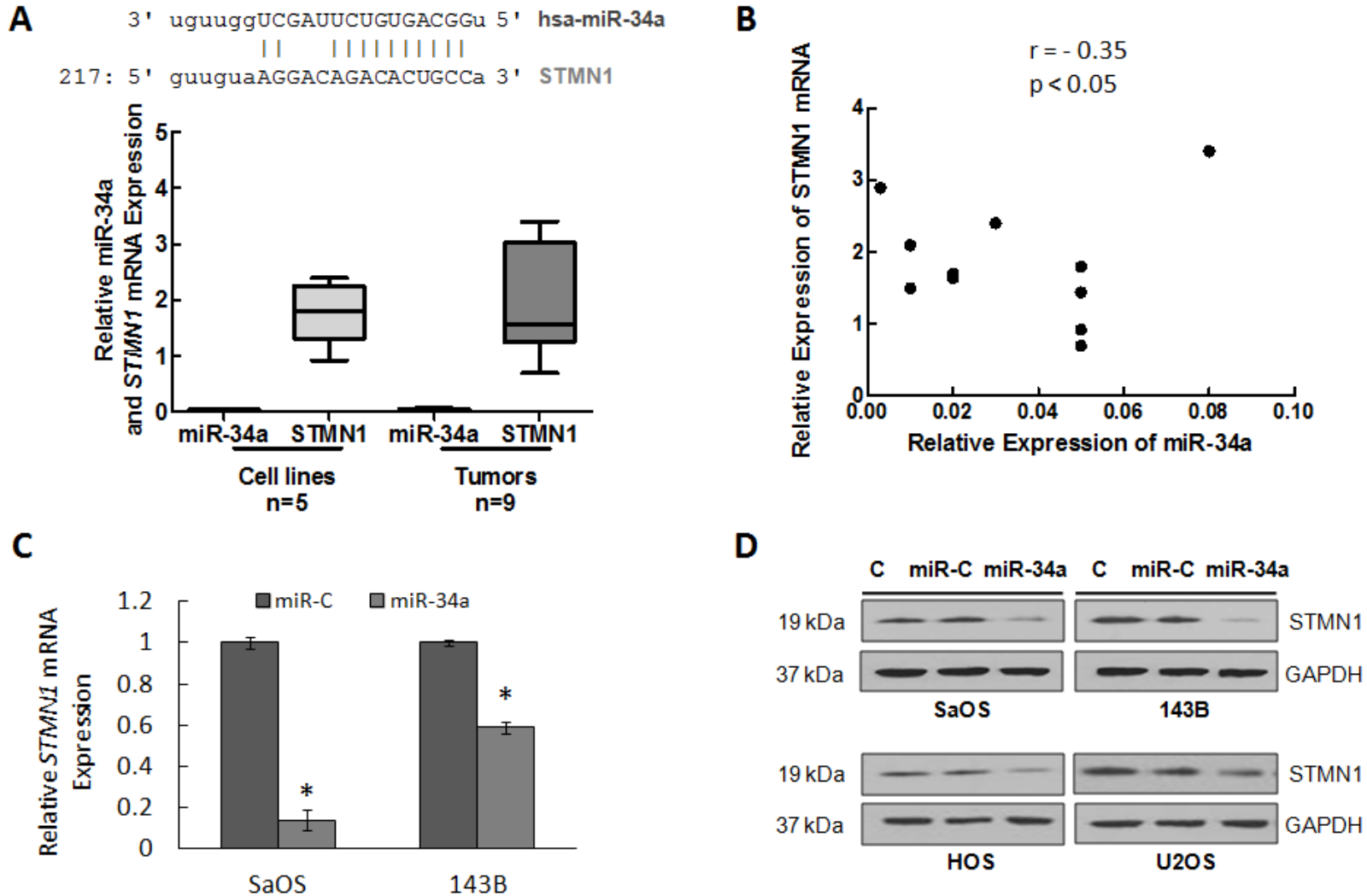
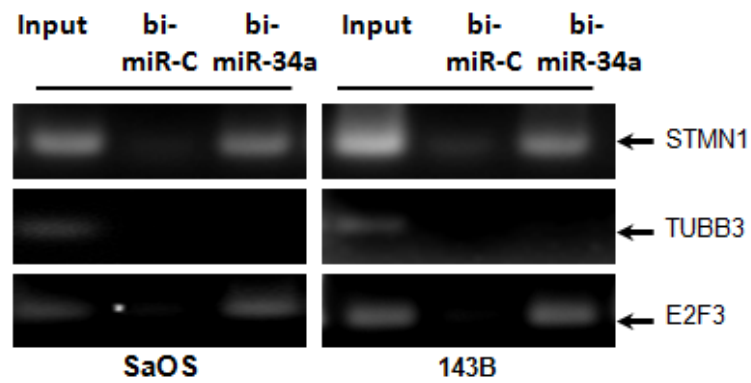
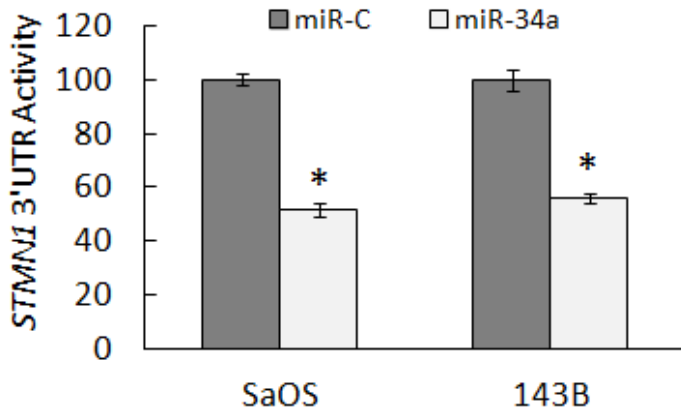


Figure 1

**A**



**B**



**C**

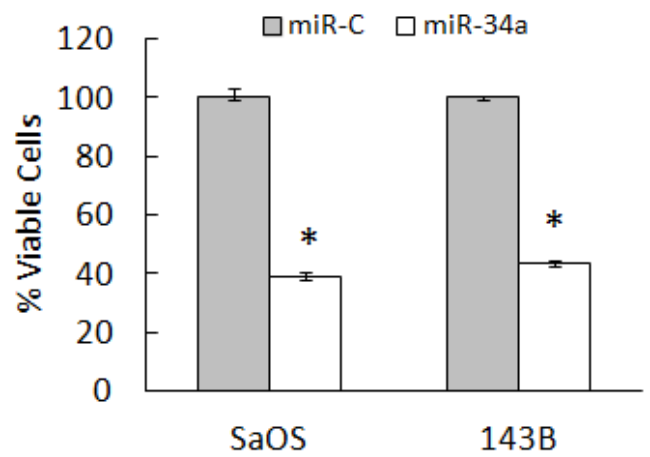


Figure 2

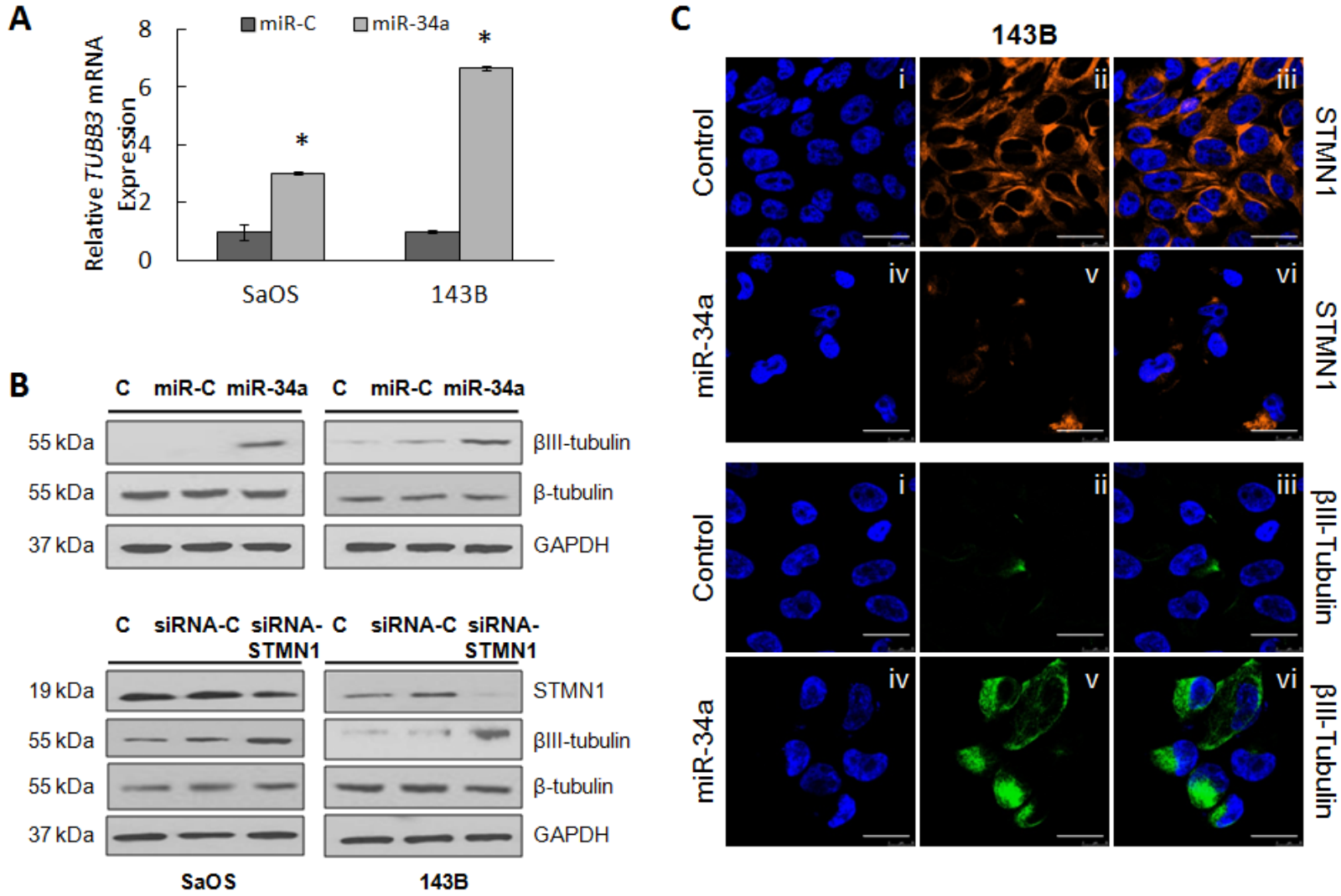


Figure 3

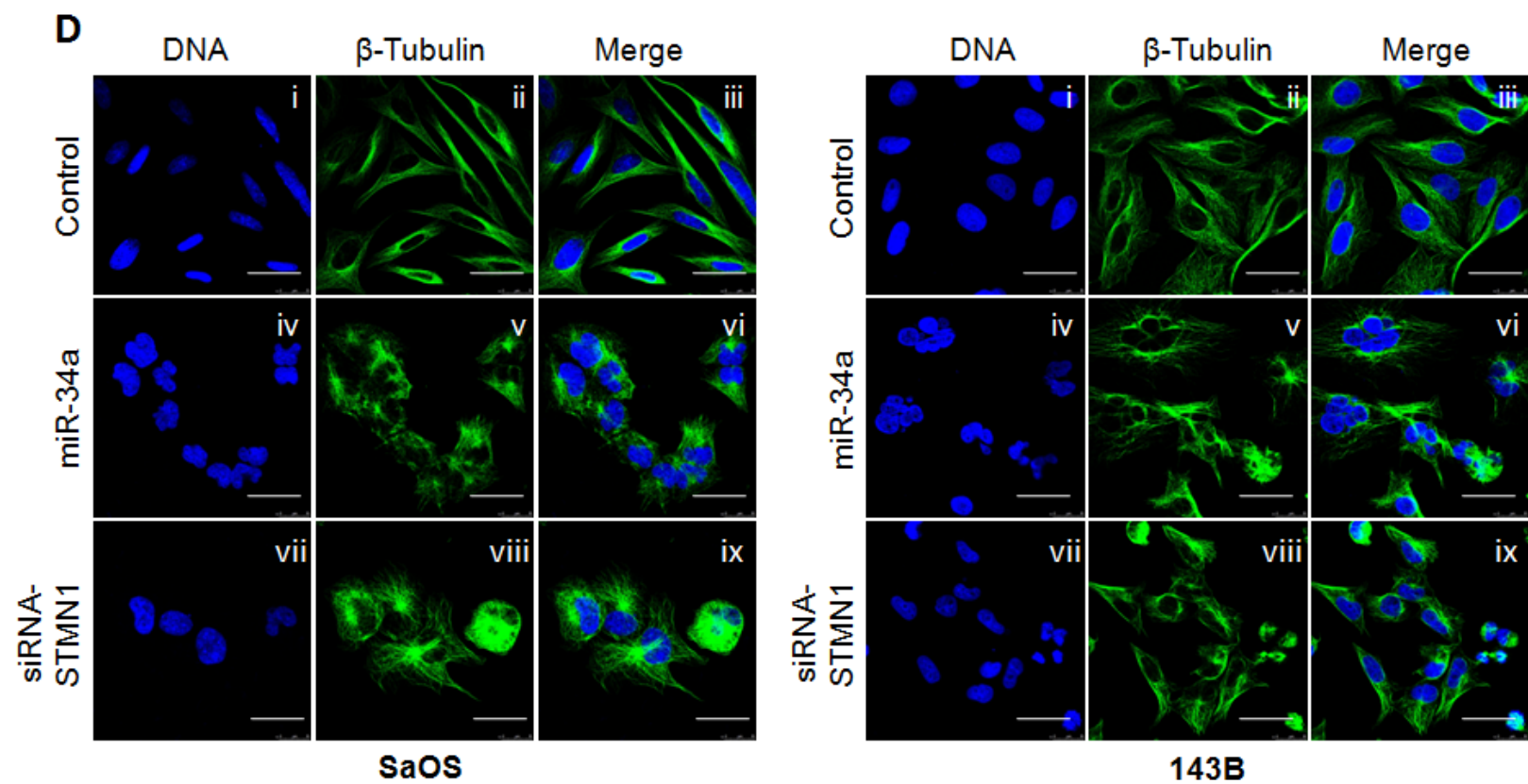
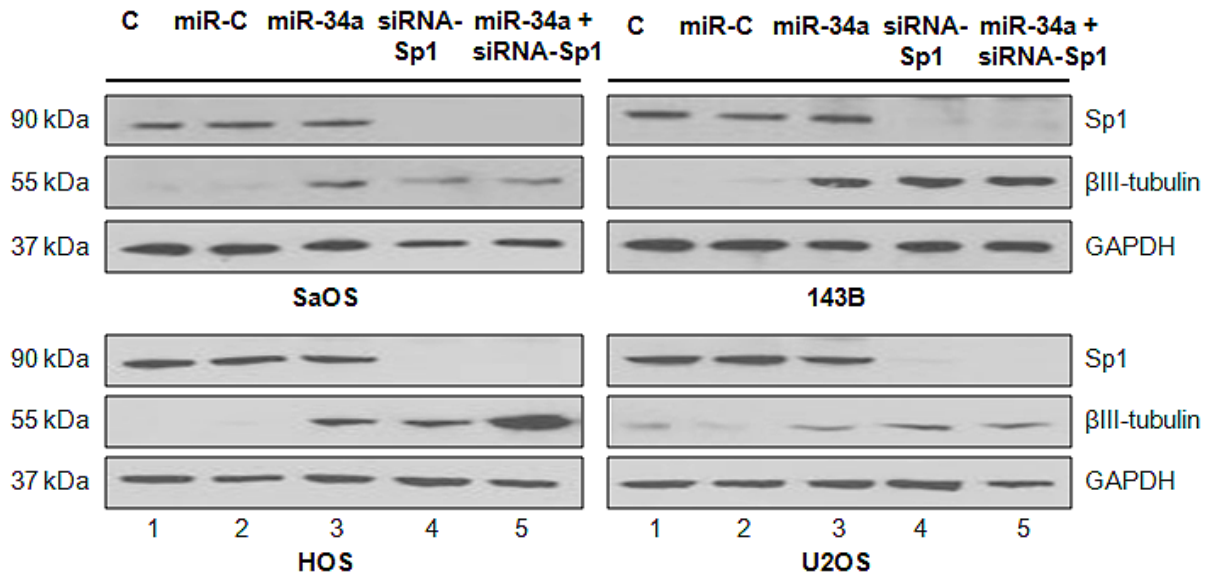


Figure 3

**A**



**B**

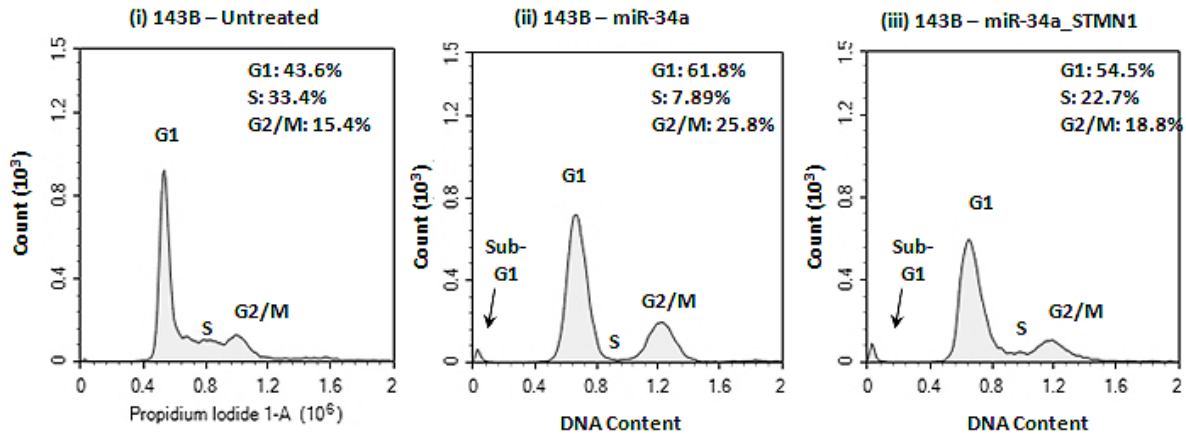
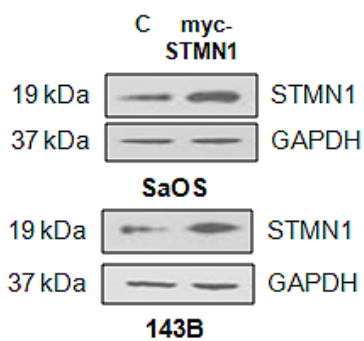
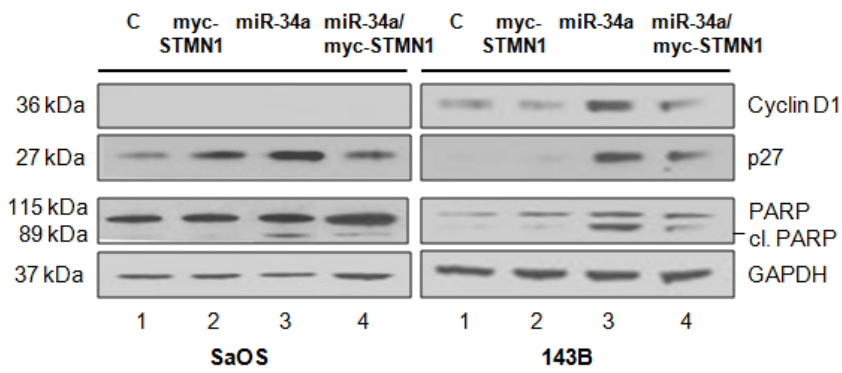


Figure 4

**C**



**D**

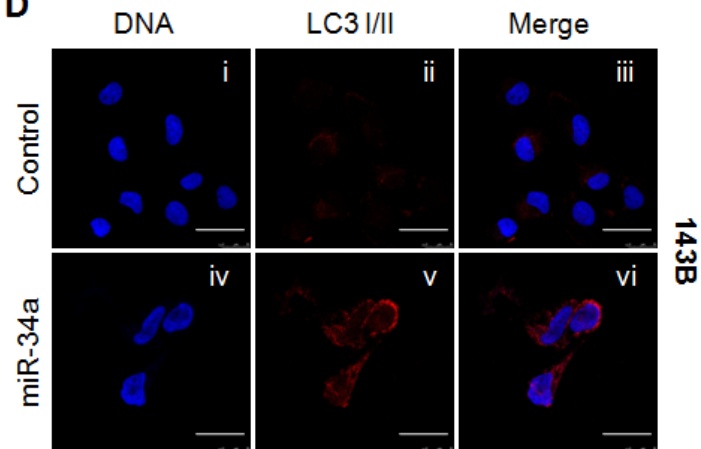


Figure 4

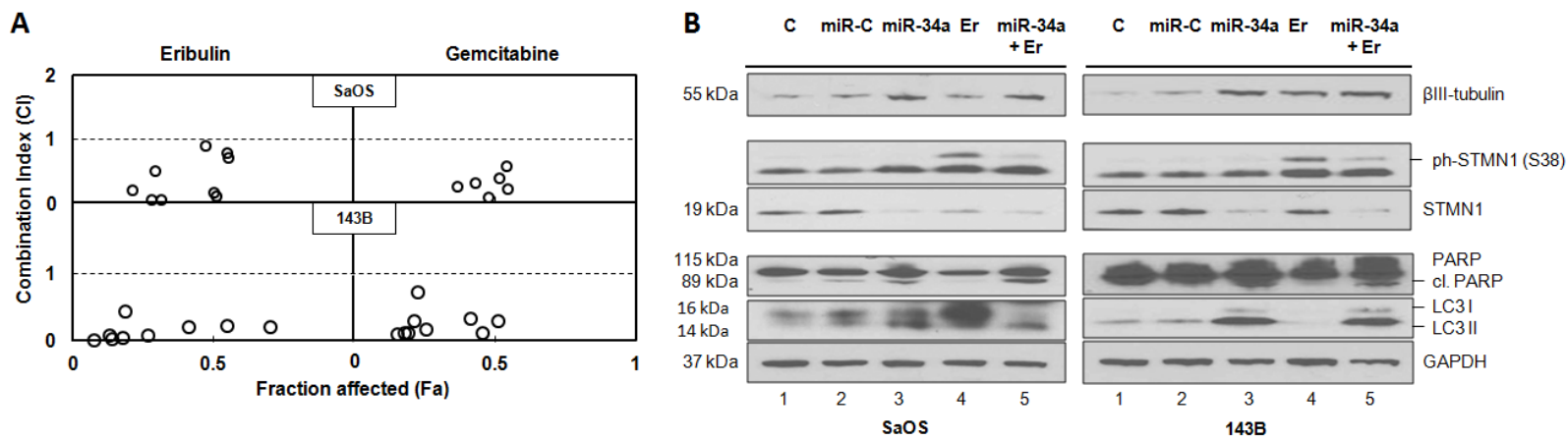


Figure 5



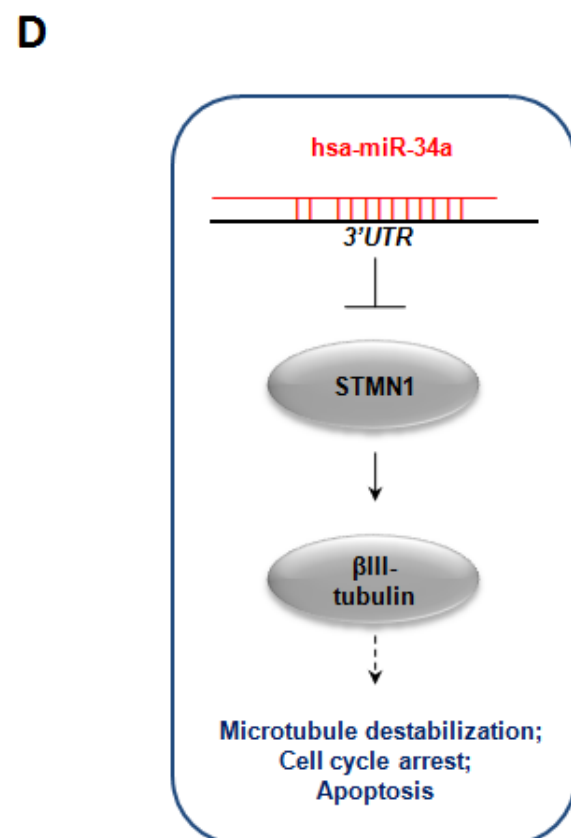
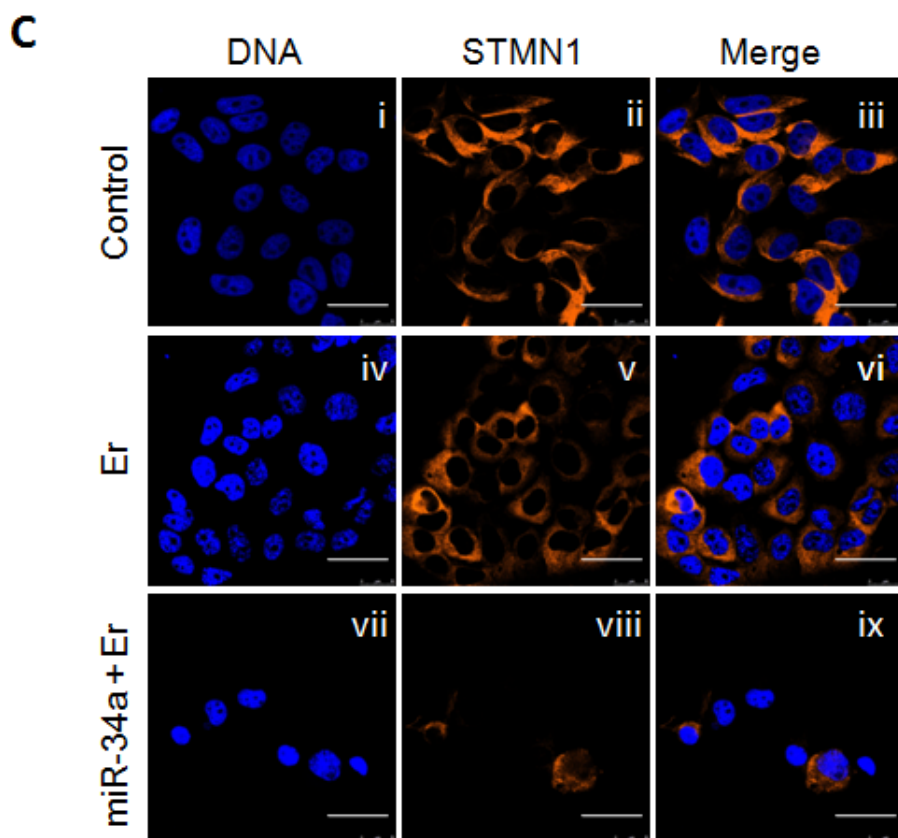


Figure 5

# Molecular Cancer Research

## The Microtubule Network and Cell Death are Regulated by a miR-34a/Stathmin 1/betall-tubulin Axis

Nancy S Vetter, E Anders Kolb, Valerie B. Sampson, et al.

*Mol Cancer Res* Published OnlineFirst March 8, 2017.

<b>Updated version</b>	Access the most recent version of this article at: doi: <a href="https://doi.org/10.1158/1541-7786.MCR-16-0372">10.1158/1541-7786.MCR-16-0372</a>
<b>Supplementary Material</b>	Access the most recent supplemental material at: <a href="http://mcr.aacrjournals.org/content/suppl/2017/03/08/1541-7786.MCR-16-0372.DC1">http://mcr.aacrjournals.org/content/suppl/2017/03/08/1541-7786.MCR-16-0372.DC1</a>
<b>Author Manuscript</b>	Author manuscripts have been peer reviewed and accepted for publication but have not yet been edited.

**E-mail alerts** [Sign up to receive free email-alerts](#) related to this article or journal.

**Reprints and Subscriptions** To order reprints of this article or to subscribe to the journal, contact the AACR Publications Department at [pubs@aacr.org](mailto:pubs@aacr.org).

**Permissions** To request permission to re-use all or part of this article, contact the AACR Publications Department at [permissions@aacr.org](mailto:permissions@aacr.org).